

Y3: N21/5:6/1713
9Un39

GOVT. DOC.

NACA TN No. 1713

NATIONAL ADVISORY COMMITTEE FOR AERONAUTICS

TECHNICAL NOTE

No. 1713

EXPERIMENTAL STUDY OF EFFECT OF VANELESS-DIFFUSER

DIAMETER ON DIFFUSER PERFORMANCE

By Guy R. Bradshaw and Eugene B. Laskin

Lewis Flight Propulsion Laboratory
Cleveland, Ohio



Washington
October 1948

GOVERNMENT LIBRARY

OCT 1 1948

BUSINESS, SCIENCE
& TECHNOLOGY DEPT.

NATIONAL ADVISORY COMMITTEE FOR AERONAUTICS

TECHNICAL NOTE No. 1713

EXPERIMENTAL STUDY OF EFFECT OF VANELESS-DIFFUSER

DIAMETER ON DIFFUSER PERFORMANCE

By Guy R. Bradshaw and Eugene B. Laskin

SUMMARY

For vaneless-diffuser diameters of 34, 27, 24, and 20 inches were studied by successively cutting down a 34-inch vaneless diffuser and running it in a variable-component rig with a commercial mixed-flow impeller to determine the variations in both compressor and diffuser efficiency with diffuser diameter. Runs were made at actual impeller tip speeds of 500 to 1300 feet per second through a range of air flows from open throttle to surge to investigate the relation between diffuser efficiency and diffuser diameter under widely varying operating conditions. Total-pressure surveys were made at several radii throughout the diffuser and these, together with the standard measurements, provided information concerning the magnitude and the location of the important losses in efficiency through the diffuser.

Substantial variations in over-all compressor performance were produced by changes in diffuser diameter; over-all compressor efficiency increased with increasing diffuser diameter. In all the diffusers, losses in efficiency were limited to the entrance and exit regions, losses in the interior of the diffusers being negligible. Diffuser-exit losses increased from 3 to 15 points as diffuser diameter decreased, the losses being approximately inversely proportional to the square of the diffuser diameter. Diffuser-entrance losses amounted to about 0.06 and showed no systematic variation with diffuser diameter. In general, mean entrance and exit losses varied only slightly with load coefficient and tip speed.

No important effects of diffuser diameter on impeller efficiency were observed.

INTRODUCTION

The vaneless diffuser, as compared with the vaned diffuser, has the desirable characteristic of a relatively flat efficiency curve

over a wider operating range but has two serious disadvantages, comparatively low peak efficiency and excessive size. Reference 1 describes a method of designing vaneless diffusers of wide operating range and presents experimental evidence that vaneless diffusers can be designed to give peak compressor efficiencies that compare favorably with those obtained by using the same impeller and the manufacturer's vaned diffuser. However, because the diameter of the vaneless diffuser is 34 inches and that of the vaned diffuser is 17, a study of the relation between vaneless-diffuser diameter and efficiency was made at the NACA Cleveland laboratory to determine whether the size could be reduced to dimensions comparable with those of the vaned diffuser without incurring prohibitive penalties in efficiency.

A duplicate of the optimum vaneless diffuser of reference 1 was therefore reduced in three successive steps from a 34-inch diameter to a diameter of 20 inches, which reduced the vaneless-diffuser diameter to about 18 percent more than that of the manufacturer's vaned diffuser.

The same impeller was used in this study as in reference 1. Each of the impeller-diffuser combinations was run over a wide range of actual tip speeds and over a range of volume flows from open throttle to surge. Pressure surveys at several radial distances along the diffusers, together with standard measurements, provided data for determining the approximate location and magnitude of energy losses in the diffuser passages.

APPARATUS AND INSTRUMENTATION

A variable-component rig (reference 2) was modified by substituting a single tangential outlet for the two radial outlets. No appreciable difference in performance resulted from this change in setup.

The commercial mixed-flow impeller (fig. 1) discharges the air with an appreciable axial component of velocity. Instead of being sharply curved at the inlet inducer section, as is characteristic of conventional impellers, the blades are designed with a gradual curvature throughout the entire length. The impeller is semi-shrouded, has 23 blades, an inlet diameter of 8.250 inches, and a tip diameter that varies axially from 11.015 to 11.241 inches. The running frontal clearance of the impeller is 0.035 inch.

The vaneless diffusers have an area expansion, along a logarithmic-spiral design path, equivalent to that of a 6° cone and a ratio of throat width to inlet width of 0.72. The largest diffuser used was the diffuser giving optimum performance in reference 1. The small diffusers were formed by successively cutting down the original diffuser of 34-inch diameter to diameters of 27, 24, and finally 20 inches. The diffuser surfaces were polished and lacquered for this series of experiments. A perspective drawing of the impeller-diffuser assembly is shown in figure 2.

In addition to the standard instrumentation P_1 and P_2 (reference 2), total-pressure tubes P_3 to P_7 were installed along the diffuser at the radii shown in figure 3. This figure also shows the total-pressure tube employed, which was a $3/32$ -inch-diameter cylindrical tube with one end plugged and rounded off and a 0.020-inch-diameter hole drilled through the wall near the plugged end. These tubes were used to establish the distribution of total pressure between the front and rear walls of the diffuser and were so located radially that each reduction in diffuser size eliminated one pressure-survey station and placed the next station $1/2$ inch from the periphery of the modified diffuser. For these pressure surveys, the total pressures at four points across the diffuser channel at each radius were determined and the arithmetical average of the four readings was taken as the total pressure at that station. These points were the midpoints of four equal cross-channel lengths.

PROCEDURE

The standard procedure for testing centrifugal superchargers was followed, runs being made for each impeller-diffuser combination from open throttle to surge at the speeds shown in the following table:

Diffuser diameter (in.)	Actual impeller tip speed (ft/sec)							
	500	700	800	900	1000	1100	1200	1300
34	X	X		X		X	X	X
27		X	X	X	X	X	X	X
24		X	X	X	X	X	X	X
20	X	X	X	X	X	X	X	X

An electric tachometer of the prescribed accuracy (reference 2) was used to measure the impeller speed, and a calibrated stroboscope provided a continuous visual check on this speed. Impeller tip speed was based on the maximum diameter of the impeller.

The total temperature was assumed to be constant throughout the diffuser and equal to the total temperature at the measuring station in the outlet duct. Ambient inlet-air temperature varied over the series of runs from 68° to 100° F.

Adiabatic efficiency was calculated from the measurements in the inlet and outlet ducts P_1 and P_2 , respectively, and from the pressure surveys at each location on each of the diffusers P_3 to P_7 . Calculations of the performance characteristics were made in accordance with the recommendations of reference 3 (where applicable) from the pressure reading at the appropriate survey station, instead of the outlet-duct pressure, in order to find the efficiency changes through the diffuser. The considerations underlying the diffuser-exit-velocity calculations are given in appendix A and the method used in finding these velocities, in appendix B.

RESULTS AND DISCUSSION

For brevity the following terms are employed in the discussion:

1. Impeller efficiency refers to the efficiency determined from pressure measurements 0.25 inch downstream of the impeller outlet (station 3).
2. Diffuser entrance refers to the region between station 3, 0.25 inch downstream of the impeller outlet (radius, 5.87 in.), and station 4 (radius, 9.5 in.).
3. Internal refers to the region between station 4 (radius, 9.5 in.) and the survey station 0.5 inch upstream of the diffuser periphery (station 4, 5, 6, or 7, depending on the diffuser).
4. Diffuser exit refers to the region between the diffuser-exit survey station (0.5 in. upstream of the diffuser periphery, station 4, 5, 6, or 7) and the measuring station in the outlet duct (station 2).

Diffuser-entrance losses do not include losses in the first 0.25 inch of the diffuser, so that impeller efficiency is penalized and diffuser efficiency exaggerated by this unknown factor. On the other hand, diffuser-entrance losses are primarily attributable to bad flow conditions at the impeller outlet caused by inefficient impeller passages and should not be charged against diffuser design even though the pressure losses actually occur in the diffuser entrance. Diffuser efficiency is penalized to the extent that

diffuser-exit losses include skin-friction losses in the outlet duct. The friction losses in the outlet duct are relatively small, however, because of the low velocities and, as they would cause no essential changes in the results, they are included with the momentum losses as diffuser-exit losses.

Impeller efficiency. - Although impeller efficiency was a secondary consideration in this study and the uncertainties of total-pressure measurements at the impeller outlet make the significance of impeller-efficiency calculations questionable, any definite trend in impeller performance with changing diffuser diameter was pertinent and a preliminary investigation of impeller efficiency was therefore undertaken.

The average value of peak impeller efficiency (over the range of tip speeds employed with each diffuser) varied from 0.91 to 0.88 and no correlation existed between diffuser diameter and impeller efficiency. Peak impeller efficiency decreased with increasing tip speed in essentially the same manner for all four diffusers, dropping from about 0.94 at an actual tip speed of 500 feet per second to 0.84 at an actual tip speed of 1300 feet per second. Impeller operating conditions with the different diffusers were not completely similar because the recommended procedure (reference 2) specifies a pressure of 40 inches of mercury absolute in the outlet duct, which necessitates a higher impeller-outlet pressure with the small diffusers than with the large ones.

Diffuser efficiency. - An over-all picture of the behavior of the four diffusers may be obtained from figure 4 for the runs at peak compressor efficiency. Adiabatic efficiencies are plotted for each of the survey stations and for the outlet duct at low, medium, and high tip speeds. Important losses occur exclusively in the diffuser-entrance and diffuser-exit regions, internal losses being relatively insignificant. Diffuser-entrance losses for peak-efficiency runs average about 8 points and their magnitude bears no relation to diffuser diameter. Qualitatively similar results were obtained in a study of vaneless-diffuser friction factors (reference 4), which indicated that the apparent friction factor at the entrance region, calculated from both total- and static-pressure measurements, was two to three times the internal friction factor. Diffuser-exit losses range from 3 to 15 points and, in general, increase as diffuser diameter decreases.

Essentially the same results are obtained if average values of the losses in the three regions of the diffuser are plotted (fig. 5).

The value plotted is the average of the losses at maximum, peak-efficiency, and minimum load coefficient for all impeller tip speeds at which the diffuser was studied. In order to reduce the effect of variations in efficiency upstream of the point under consideration, losses are shown as percentages of the efficiency at that point, that is, entrance losses in percentage of impeller-outlet efficiency, internal losses in percentage of diffuser-entrance efficiency, and diffuser-exit losses in percentage of diffuser-exit efficiency. Average diffuser-entrance losses are approximately constant at about 6 percent. The apparent increase with diffuser diameter is probably insignificant in view of the inaccuracies of impeller-exit measurements. Average internal losses, always small, increased slowly with increasing diffuser diameter, as would be expected from the increased length of flow path. Average diffuser-exit losses increased from 3 to 13 percent as the diffuser diameter was reduced from 34 to 20 inches.

Entrance losses. - The behavior of entrance losses with varying load coefficient is shown for the four diffusers (fig. 6) for three impeller tip speeds, together with the mean value over the three speeds for each of the diffusers. The variations in efficiency loss with load coefficient appear to be small and erratic and no significant differences exist in the behavior of the different diffusers.

The mean variations in entrance losses with impeller tip speed for the four diffusers are shown in figure 7. Values plotted are, for a given diffuser, the minimum, peak-efficiency, and maximum load coefficients and the average of these three. The behavior of all the diffusers is qualitatively similar, mean losses being essentially constant up to a tip speed of about 900 feet per second and then increasing slowly with tip speed. In general, the losses at the high tip speeds are somewhat greater for the larger-diameter diffusers.

Exit losses. - The variations in diffuser-exit losses with load coefficient for the four diffusers are shown in figure 8 for three impeller tip speeds together with the mean values for the three speeds for each diffuser. For all the diffusers, exit losses increase slightly with load coefficient, the rate of increase being almost linear and about the same for all diameters. Absolute values of exit losses increase in approximately inverse proportion to the square of the diffuser diameter. The over-all efficiency of the compressor is accordingly reduced as the diffuser diameter is reduced.

In general, exit losses decrease slightly with increasing tip speed (fig. 9). The rate of decrease is essentially constant in most cases and appears to increase with decreasing diffuser diameter.

Diffuser-exit velocity. - The velocity at the diffuser exit is pertinent in that it affords a basis for estimating the losses that may be expected in the collector. The exit velocities were calculated (appendix B) for each diffuser and plotted against load coefficient (fig. 10) for the different tip speeds.

The delivery velocities of the four diffusers and the corresponding dynamic pressures for an actual tip speed of 1100 feet per second, a design load coefficient of 0.26, and an outlet-duct total pressure of 40 inches of mercury absolute are presented in the following table:

Diffuser diameter (in.)	Exit velocity (ft/sec)	Dynamic pressure (in. Hg)	Pressure loss with 80-percent-efficient collector (in. Hg)
34	237	0.95	0.19
27	327	1.86	.37
24	378	2.54	.51
20	488	4.36	.87

If a collector having an efficiency of 80 percent is assumed, the pressure losses at the diffuser exit would be as shown in the fourth column. With this hypothetical collector, the gain with a 34-inch instead of a 20-inch diffuser would be only about 0.7 inch of mercury absolute. This pressure increment is equivalent to a gain in over-all efficiency of 0.016. With such a collector, the diffuser diameter would therefore depend primarily on the exit velocity desired.

General discussion. - Because of the chaotic flow at the impeller outlet, the diffuser-entrance region is precisely that portion of the diffuser for which no detailed design theory is possible. With the present information, the losses in this region may be largely unavoidable until the flow from the impeller is improved. On the other hand, the flow at the diffuser exit is relatively steady and it should be possible to design a transition section through this region that would reduce exit losses to the point where a small vaneless diffuser would permit compressor operation at satisfactory efficiencies.

SUMMARY OF RESULTS

An experimental study in a variable-component rig of four vaneless diffusers of different diameters over a range of tip speeds from 500 to 1300 feet per second and air flows from open throttle to surge gave the following results:

1. Important losses in efficiency occurred in the vicinity of the diffuser entrance and exit, internal losses being comparatively negligible.

2. Diffuser-entrance losses were approximately constant at about 6 percent, for all diameters. Diffuser-exit losses increased from 3 to 15 points as diffuser diameter decreased, the losses being approximately inversely proportional to the square of the diffuser diameter. The over-all efficiency of the compressor is therefore reduced as the diffuser diameter is reduced.

3. The effect of diffuser diameter on diffuser-entrance losses, internal losses in the diffuser, and impeller efficiency was slight.

4. Variations in load coefficient and in impeller tip speed produced comparatively small changes in diffuser efficiency and the changes are, in general, similar for diffusers of different diameters.

Lewis Flight Propulsion Laboratory,
National Advisory Committee for Aeronautics,
Cleveland, Ohio, June 24, 1948.

APPENDIX A

DETERMINATION OF FLOW CONDITIONS IN VANELESS DIFFUSER

Symbols

The following symbols are used in the appendixes (see fig. 11 for geometrical relations between velocities and dimensions):

b	distance between diffuser walls normal to rear shroud
c_p	specific heat at constant pressure
D	hydraulic diameter
f	friction factor
g	acceleration of gravity
H	total enthalpy
h	distance between diffuser walls measured parallel to impeller axis
l	distance measured along flow path
M	Mach number (ratio of V to local speed of sound)
P	total pressure
p	static pressure
R	gas constant
r	radial distance from impeller axis
T	total temperature
t	static temperature
U	impeller tip speed
V	velocity of air in diffuser
V_a	axial component of air velocity

- V_m meridional component of air velocity
 V_r radial component of air velocity
 V_θ circumferential component of air velocity
 W weight flow
 α flow angle (angle between V and V_θ)
 β angle between diffuser rear shroud and radial direction
 γ ratio of specific heats
 ρ mass density

Subscripts:

- e diffuser exit
 o impeller outlet
 2 outlet-duct measuring station

Analysis

From reference 1 (p. 19) in the notation of the present report,

$$\frac{dP}{P} = - \frac{4fV^2 dl}{2gDRt} \quad (1)$$

If the values for dl , D , and t suggested in reference 1 for a mixed-flow vaneless diffuser are substituted in equation (1), it becomes

$$\frac{dP}{P} = - \frac{fV^2 \csc \alpha dr}{gb \cos \beta RT \left(1 - \frac{V^2}{2gc_p T} \right)} \quad (2)$$

With the geometrical relation $\csc \alpha = V/V_m$, equation (2) becomes

$$\frac{dP}{P} = - \frac{fV^3 dr}{gV_m brT \cos \beta \left(1 - \frac{V^2}{2gc_p T} \right)} \quad (3)$$

Because no measurements except total pressures were taken in the diffuser, the only velocity susceptible of approximation is the circumferential component $V_{\theta,0}$ at the impeller tip, which can be estimated from the equation

$$V_{\theta,0} = \frac{g\Delta H}{U} = \frac{gc_p \Delta T}{U} \quad (4)$$

where ΔT is the difference in total temperature between the compressor inlet and outlet measuring stations.

The following equations will also be used:

1. Principle of angular momentum (reference 4)

$$\frac{d(rV_{\theta})}{rV_{\theta}} = - f \frac{V}{V_m} \frac{dr}{b \cos \beta} \quad (5)$$

in the present notation. (The fact that in the general cases the diffuser walls are inclined to planes perpendicular to the axis is considered.)

2. Equation of continuity

$$W = 2\pi r h \rho V_r g \quad (6)$$

3. Velocity relation

$$V^2 = V_{\theta}^2 + V_r^2 \sec^2 \beta \quad (7)$$

4. Density relation

$$\rho = \frac{P}{gRT} \left(1 - \frac{V^2}{2gc_p T} \right)^{\frac{1}{\gamma-1}} \quad (8)$$

993

5. Energy relation

$$T = T_0 = \text{constant} \quad (9)$$

From the values of $V_{\theta,0}$, T_0 , P_0 , and W the complete state of the gas at the impeller tip can be estimated by means of the equations

$$V_{m,0}' = \frac{W}{2\pi r_0 h_0 \rho_{t,0} \cos \beta_0}$$

(where $\rho_{t,0}$ is the stagnation density at the impeller exit and the prime is used to indicate that this velocity is calculated in terms of this density)

$$V_{r,0} = V_{m,0}' \cos \beta_0 \left(1 - \frac{V_0^2}{2gc_p T_0} \right)^{-\frac{1}{\gamma-1}}$$

$$V_0^2 = V_{\theta,0}^2 + \frac{(V_{m,0}')^2}{\left(1 - \frac{V_0^2}{2gc_p T_0} \right)^{\frac{2}{\gamma-1}}}$$

and

$$\rho_0 = \frac{\rho_{t,0}}{\left(1 - \frac{V_0^2}{2gc_p T} \right)^{-\frac{1}{\gamma-1}}}$$

When the solution of equations (3) to (9) is applied to the data, the equations are rewritten in terms of ratios of the quantities to the corresponding values at the impeller tip. If the quantities A and B are used for

$$A = \frac{V_{r,0}}{V_0 \cos \beta_0}$$

and

$$B = \frac{fV_0 r_0}{V_{r,0} \cos \beta_0 h_0} = \frac{f \sec^2 \beta_0 r_0}{h_0 A}$$

the following equations result:

$$\frac{V^2}{V_0^2} = (1-A^2) \frac{V_{\theta}^2}{V_{\theta,0}^2} + A^2 \frac{\rho_0^2 h_0^2 r_0^2 \cos^2 \beta_0}{\rho^2 h^2 r^2 \cos^2 \beta} \quad (10)$$

$$\frac{\rho}{\rho_0} = \frac{P}{P_0} \left[1 + \frac{\gamma-1}{2} M_0^2 \left(1 - \frac{V^2}{V_0^2} \right) \right]^{\frac{1}{\gamma-1}} \quad (11)$$

$$\frac{P_0}{P} = 1 + B \gamma M_0^2 \int_1^{r/r_0} \frac{rV^3 \cos \beta_0}{r_0 V_0^3 \cos \beta} \left[1 + \frac{\gamma-1}{2} M_0^2 \left(1 - \frac{V^2}{V_0^2} \right) \right]^{\frac{2-\gamma}{\gamma-1}} d\left(\frac{r}{r_0}\right) \quad (12)$$

$$\frac{V_{\theta}}{V_{\theta,0}} = \frac{r_0}{r} \exp \left[-B \int_1^{r/r_0} \frac{r\rho V \cos \beta_0}{r_0 \rho_0 V_0 \cos \beta} d\left(\frac{r}{r_0}\right) \right] \quad (13)$$

These equations may be solved by successive approximations. A first approximation is made to the velocity ratio V/V_0 by using the equation

$$\frac{V^2}{V_0^2} = \frac{r_0^2}{r^2} \left\{ (1-A^2) \exp \left[-2B \left(\frac{r}{r_0} - 1 \right) \right] + A^2 \frac{h_0^2 \cos^2 \beta_0 \left[1 + B\gamma M_0^2 \left(\frac{r}{r_0} - 1 \right) \right]^2}{h^2 \cos^2 \beta \left[1 + \frac{\gamma-1}{2} M_0^2 \left(1 - \frac{r_0^2}{r^2} \right) \right]^{\frac{2}{\gamma-1}}} \right\} \quad (14)$$

which is an approximate form of equation (10). With this value of V/V_0 , the integrand of equation (11) can be plotted and P_0/P determined graphically. A value for ρ/ρ_0 may then be obtained from equation (12) and, by graphical solution of equation (13), $V_\theta/V_{\theta,0}$ is found. This value may then be used in equation (10) to find a second approximation to V^2/V_0^2 and, from the second approximation to $V_\theta/V_{\theta,0}$, a third approximation to V^2/V_0^2 can be made if desired. This computation is unnecessary for every point for which the flow is sought; the solution may be obtained for selected values of A and M_0 (B is determined by each value of A) and the results plotted. For particular conditions of flow, a graphical solution may therefore be readily obtained.

APPENDIX B

DETERMINATION OF DISCHARGE VELOCITY IN VANELESS DIFFUSER
BY METHOD OF PRESSURE LOSS

If all the velocity pressure at the diffuser exit is assumed to be lost in a totally inefficient variable-component collector, the total pressure in the outlet duct is equal to the static pressure at the diffuser exit. No heat transfer is assumed so that the total temperature measured in the outlet duct is that at the diffuser exit. (See appendix A for definition of symbols.)

The equation

$$\frac{t_e}{T_e} = 1 - \frac{V_e^2}{2gc_p T_e} = \left(\frac{P_e}{P_2}\right)^{\frac{\gamma-1}{\gamma}}$$

solved for V_e^2 yields

$$V_e^2 = 2gc_p T_e \left[1 - \left(\frac{P_e}{P_2}\right)^{\frac{\gamma-1}{\gamma}} \right]$$

When P_2 is substituted for p_e and the equation simplified by making the additional substitution

$$Y = \left[\left(\frac{P_e}{P_2}\right)^{\frac{\gamma-1}{\gamma}} - 1 \right]$$

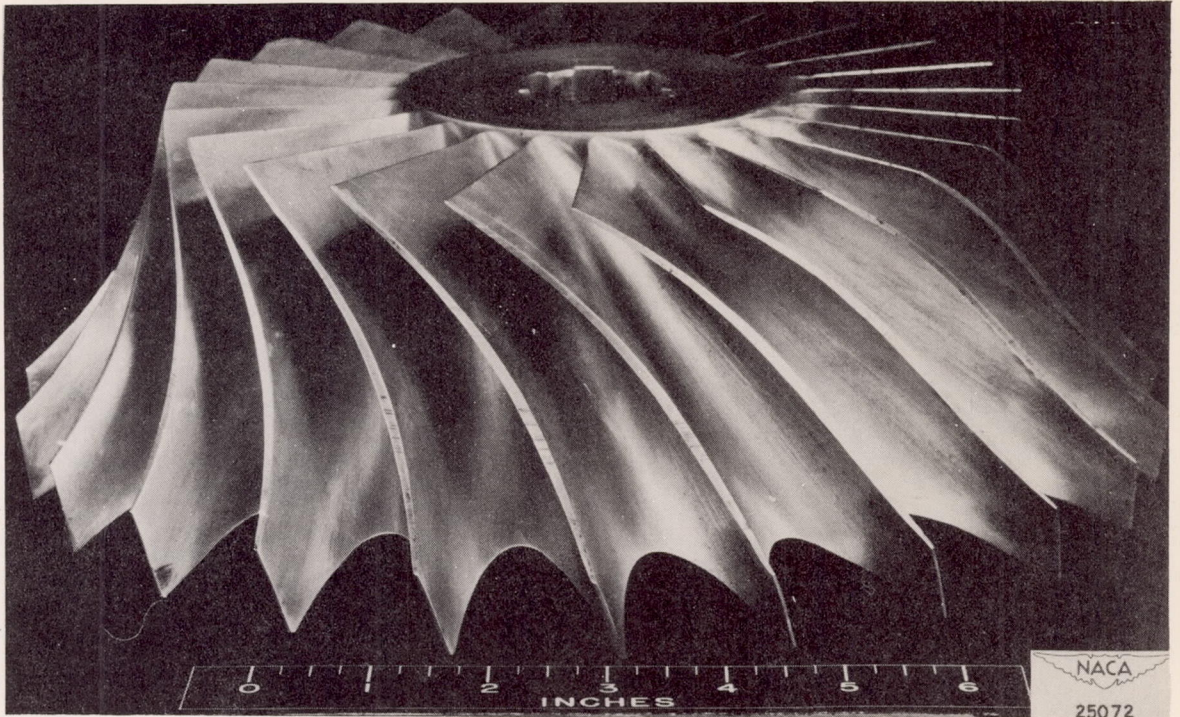
the equation for V_e becomes

$$V_e = \left[2gc_p T_e \left(\frac{Y}{1+Y} \right) \right]^{1/2}$$

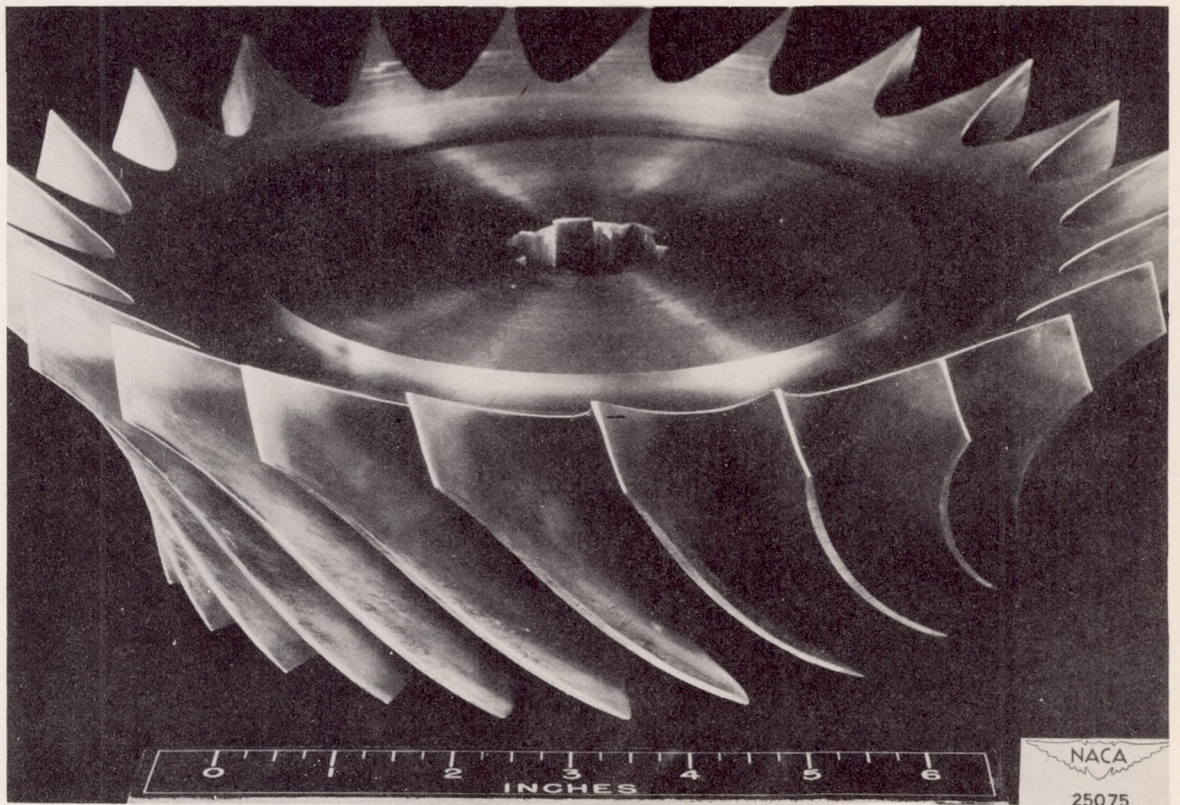
REFERENCES

1. Brown, W. Byron, and Bradshaw, Guy R.: A Method of Designing Vaneless Diffusers and Experimental Investigation of Certain Undetermined Parameters. NACA TN No. 1426, 1947.
2. NACA Subcommittee on Supercharger Compressors: Standard Procedures for Rating and Testing Centrifugal Compressors. NACA ARR No. ESF13, 1945.
3. Ellerbrock, Herman H., Jr., and Goldstein, Arthur W.: Principles and Methods of Testing Centrifugal Superchargers. NACA ARR, Feb. 1942.
4. Brown, W. Byron: Friction Coefficients in a Vaneless Diffuser. NACA TN No. 1311, 1947.

993



(a) Top view.



(b) Bottom view.

Figure 1. - Mixed-flow impeller for which vaneless diffusers were designed.

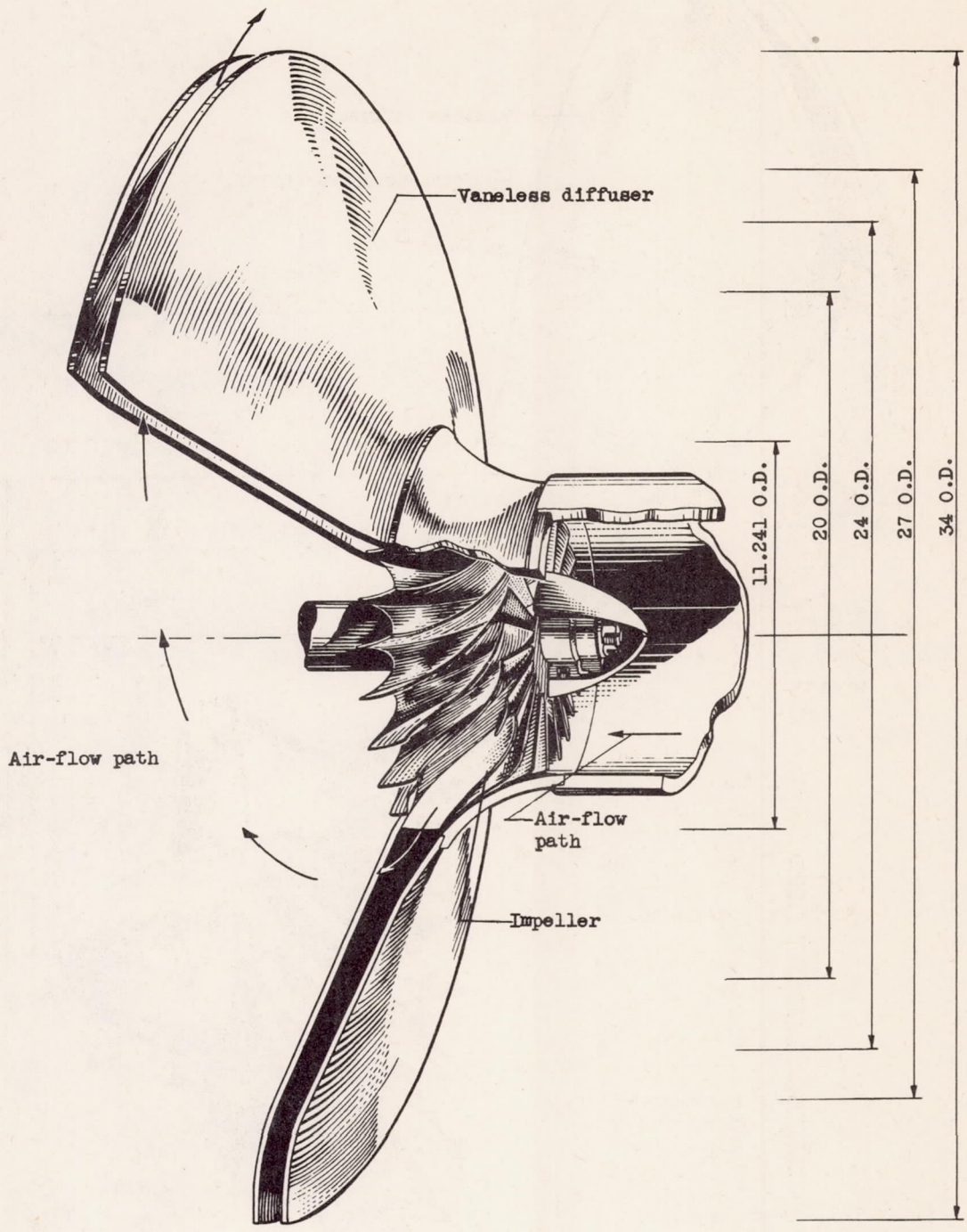


Figure 2. - Assembly of vaneless diffusers with mixed-flow impeller. (All dimensions in inches.)

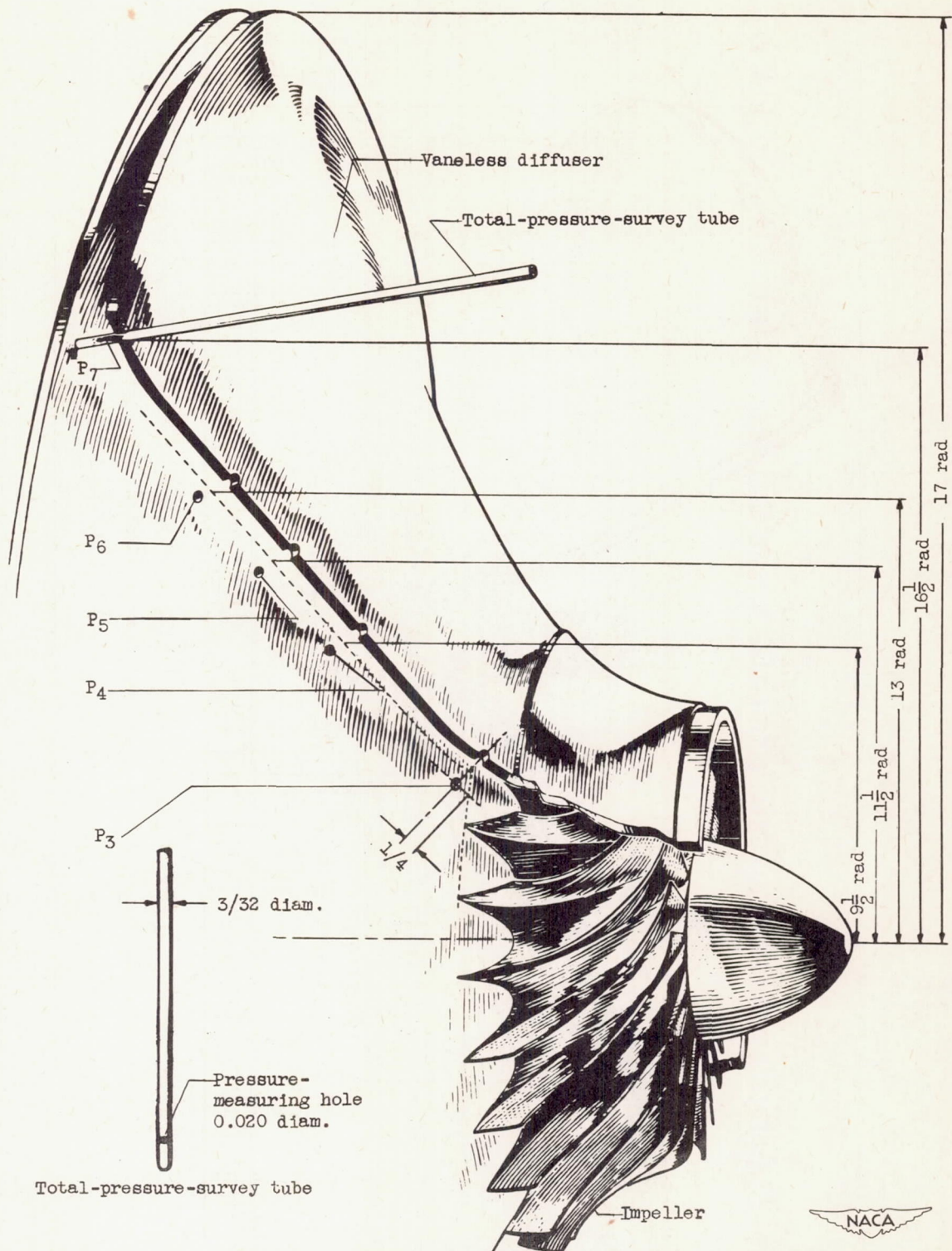
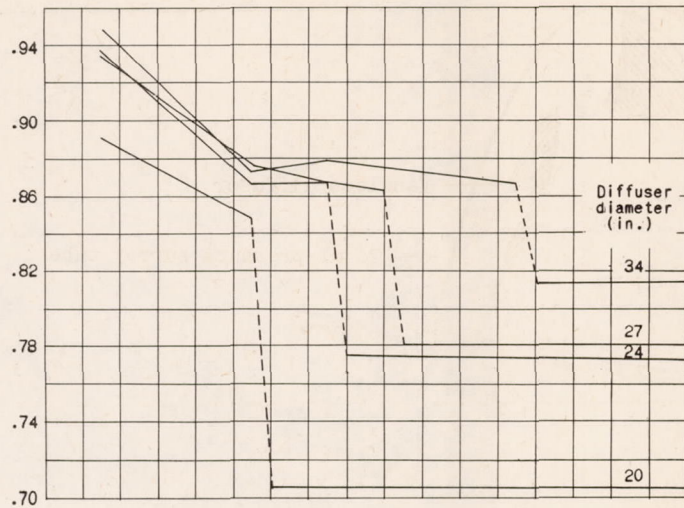
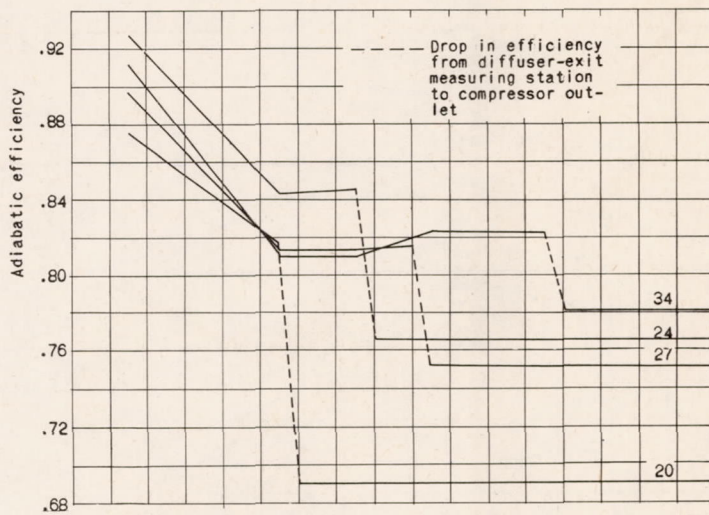


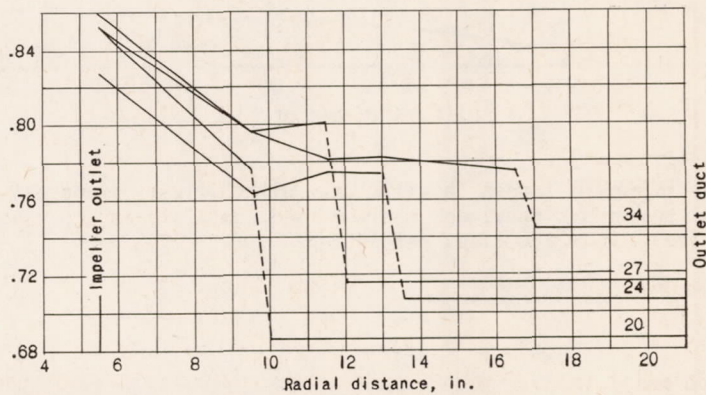
Figure 3. - Location and detail of total-pressure-survey tubes in vaneless diffuser. (All dimensions in inches.)



(a) Actual tip speed, 700 feet per second.



(b) Actual tip speed, 1100 feet per second.



(c) Actual tip speed, 1300 feet per second.

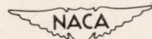


Figure 4. - Efficiency at various distances along diffuser radius and in outlet duct for peak-efficiency point.

993

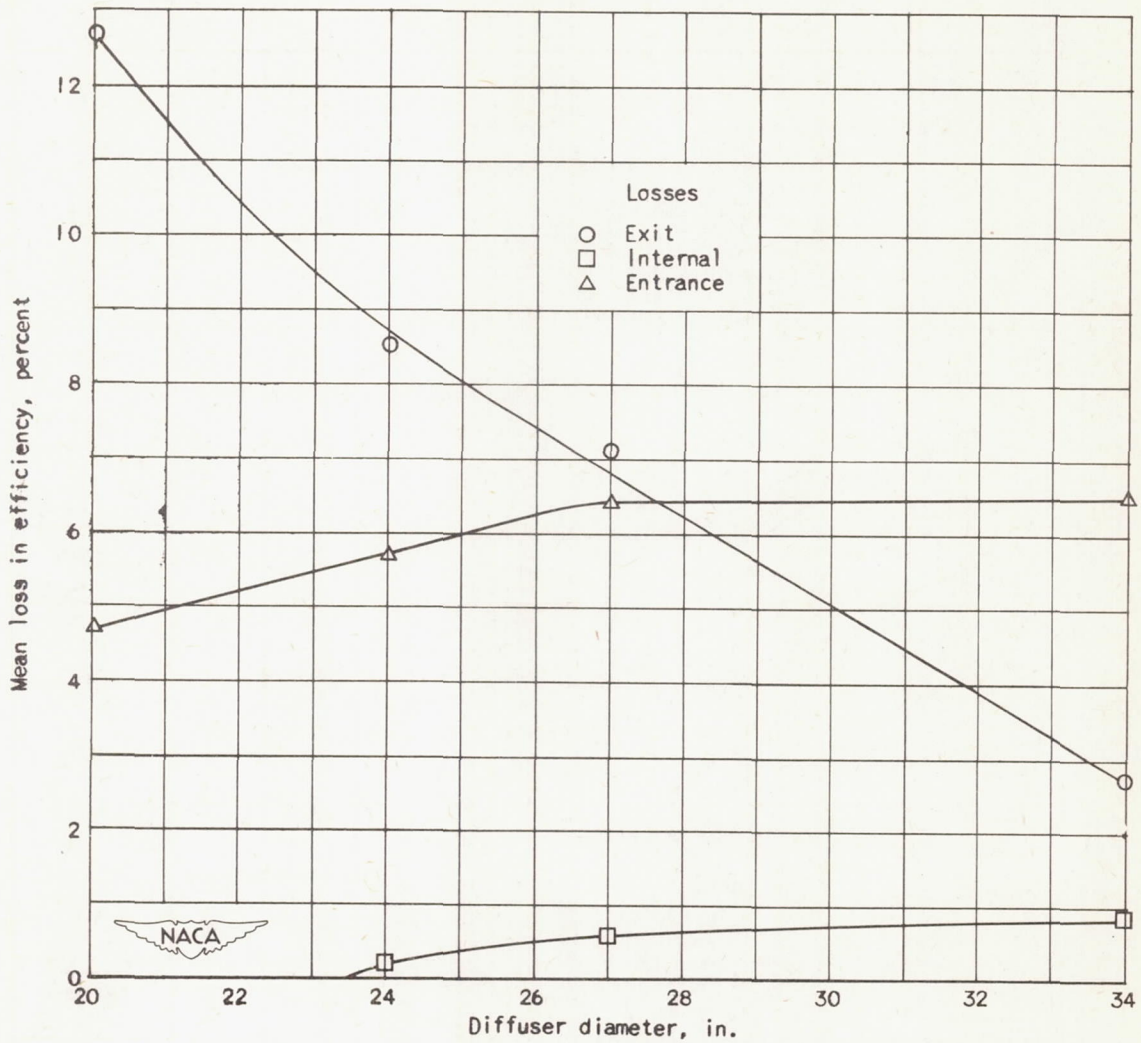


Figure 5. - Variation of losses in efficiency with diffuser diameter: average values for maximum, peak-efficiency, and minimum load coefficients and range of actual tip speeds from 700 to 1300 feet per second.

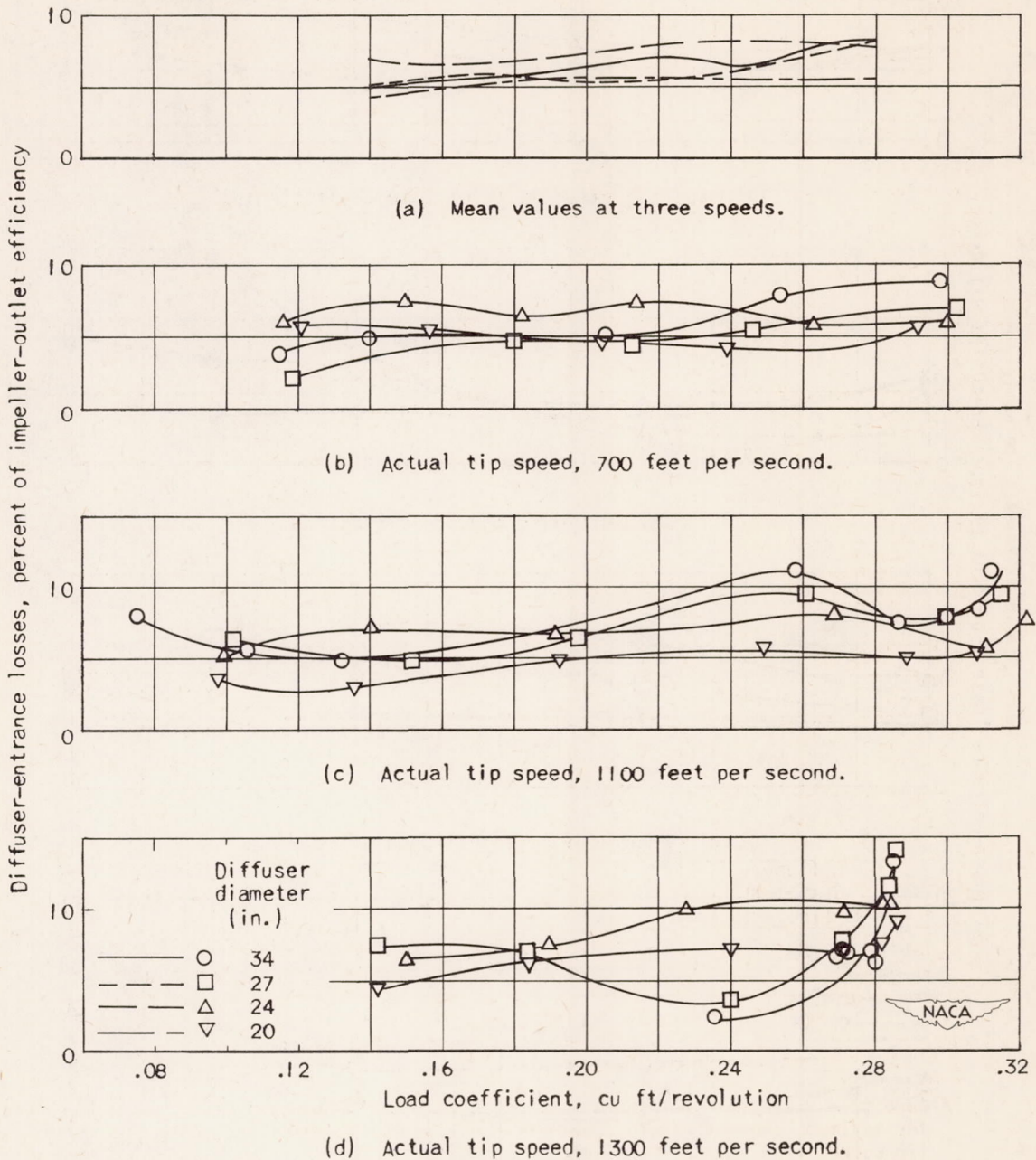


Figure 6. - Variation of diffuser-entrance losses with load coefficient.

993

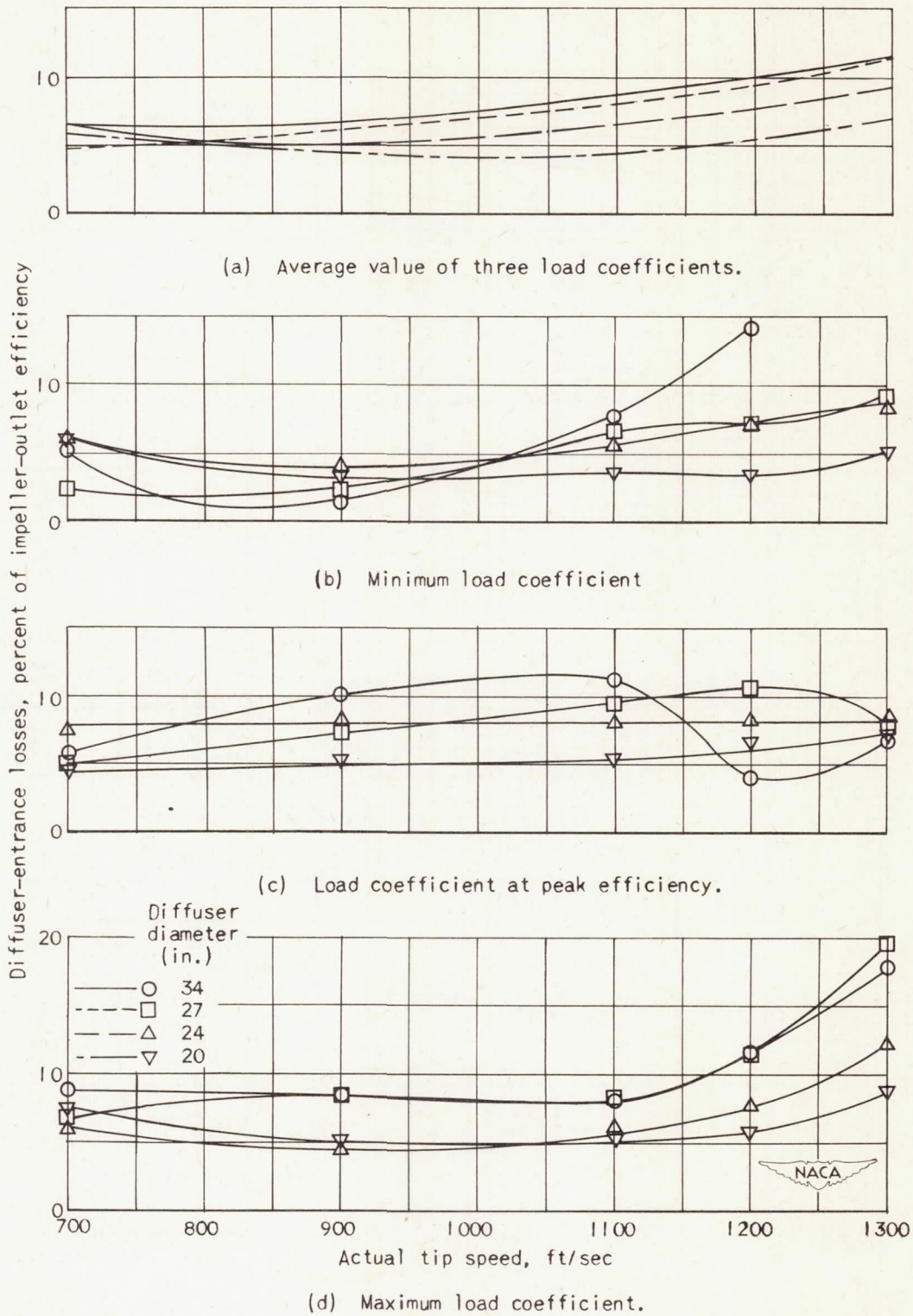
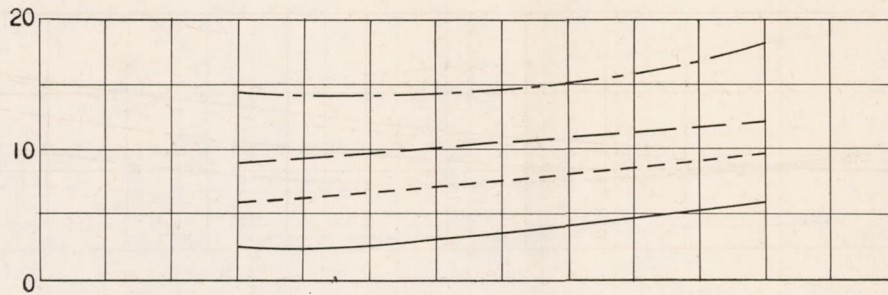
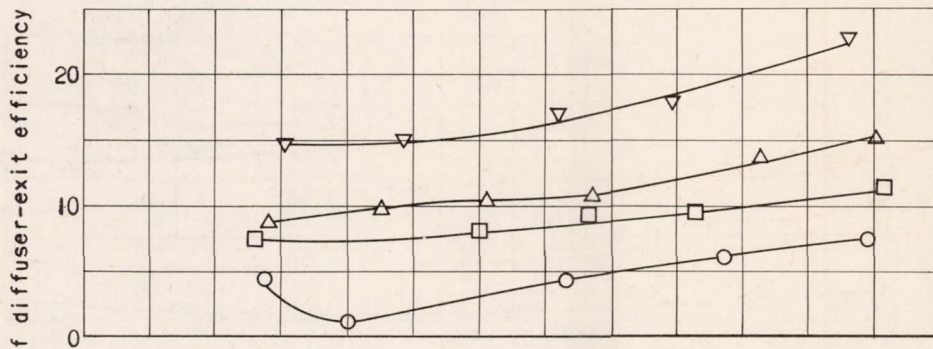


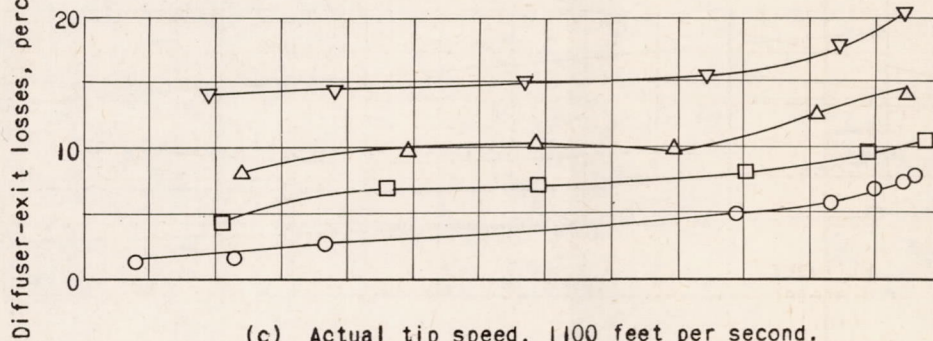
Figure 7. - Variation of diffuser-entrance losses with actual tip speed.



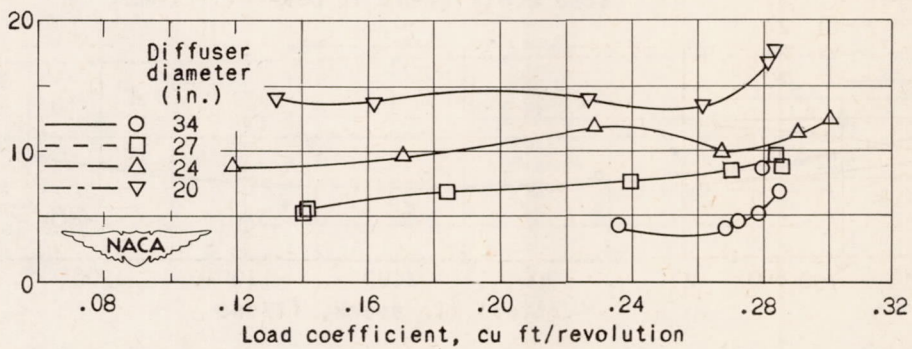
(a) Average of three actual tip speeds.



(b) Actual tip speed, 700 feet per second.



(c) Actual tip speed, 1100 feet per second.



(d) Actual tip speed, 1300 feet per second.

Figure 8. - Variation of diffuser-exit losses with load coefficient.

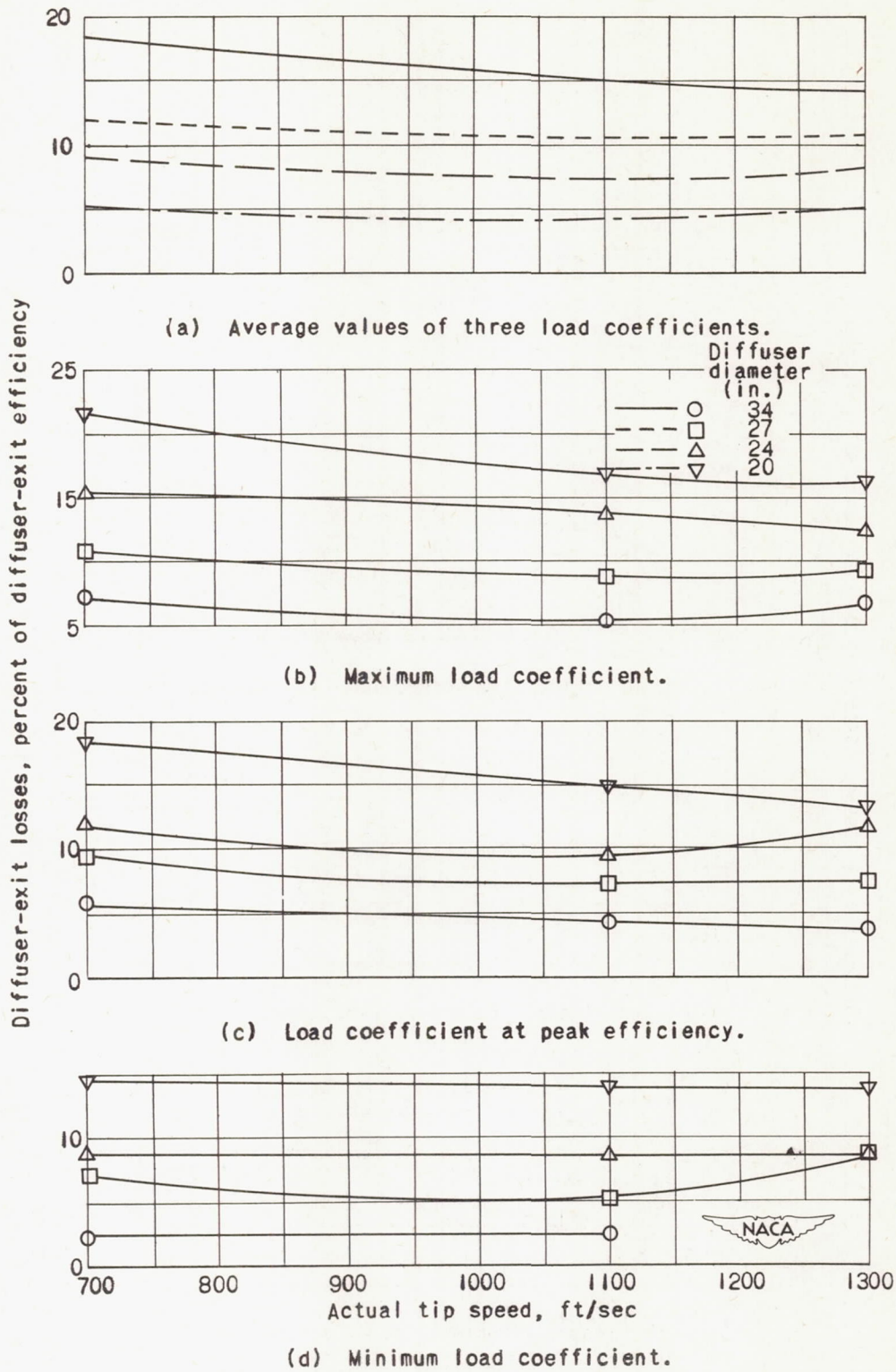
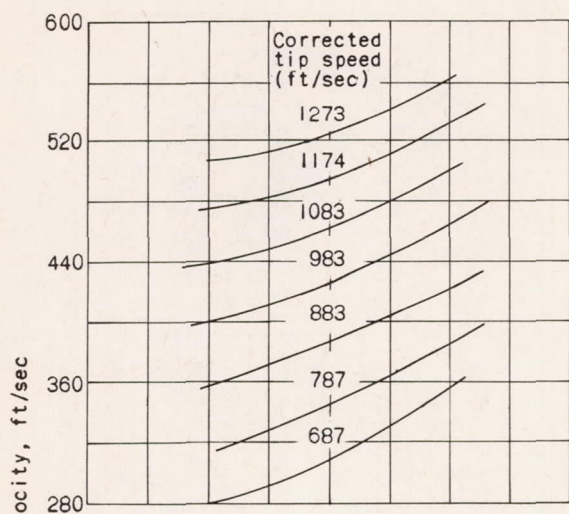
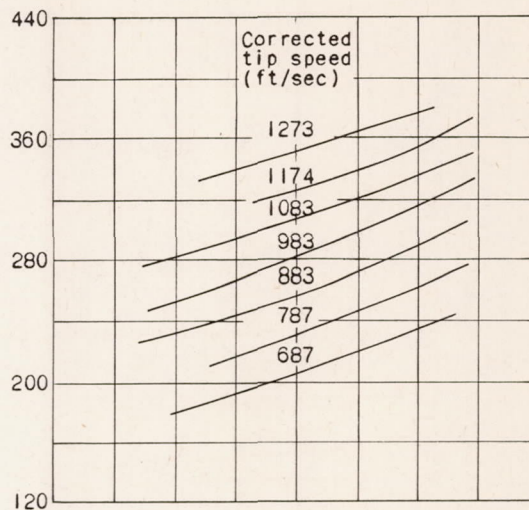


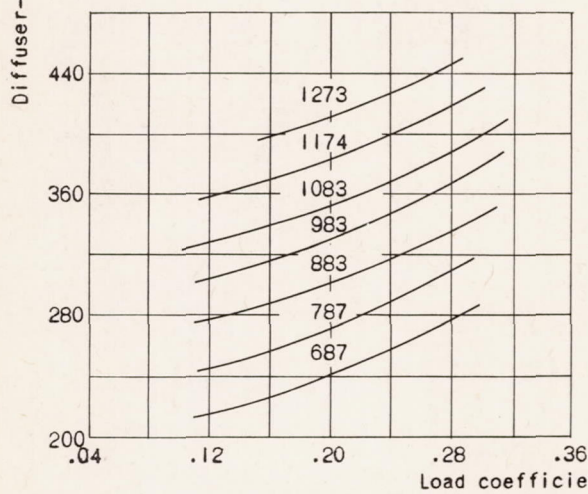
Figure 9. - Variation of diffuser-exit losses with actual tip speed.



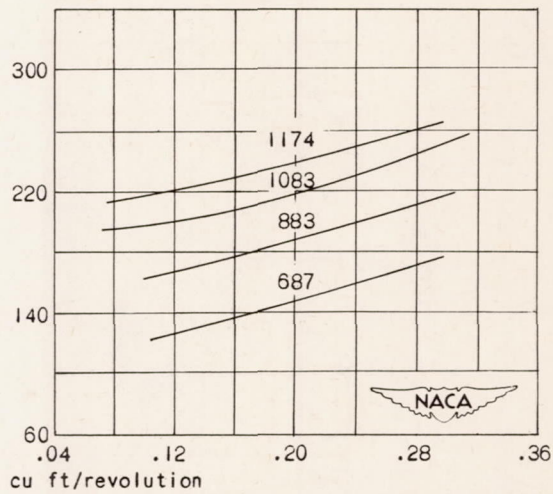
(a) Diffuser diameter, 20 inches.



(c) Diffuser diameter, 27 inches.



(b) Diffuser diameter, 24 inches.



(d) Diffuser diameter, 34 inches.

Figure 10. - Velocities at vaneless-diffuser exits calculated by method of appendix B.

993

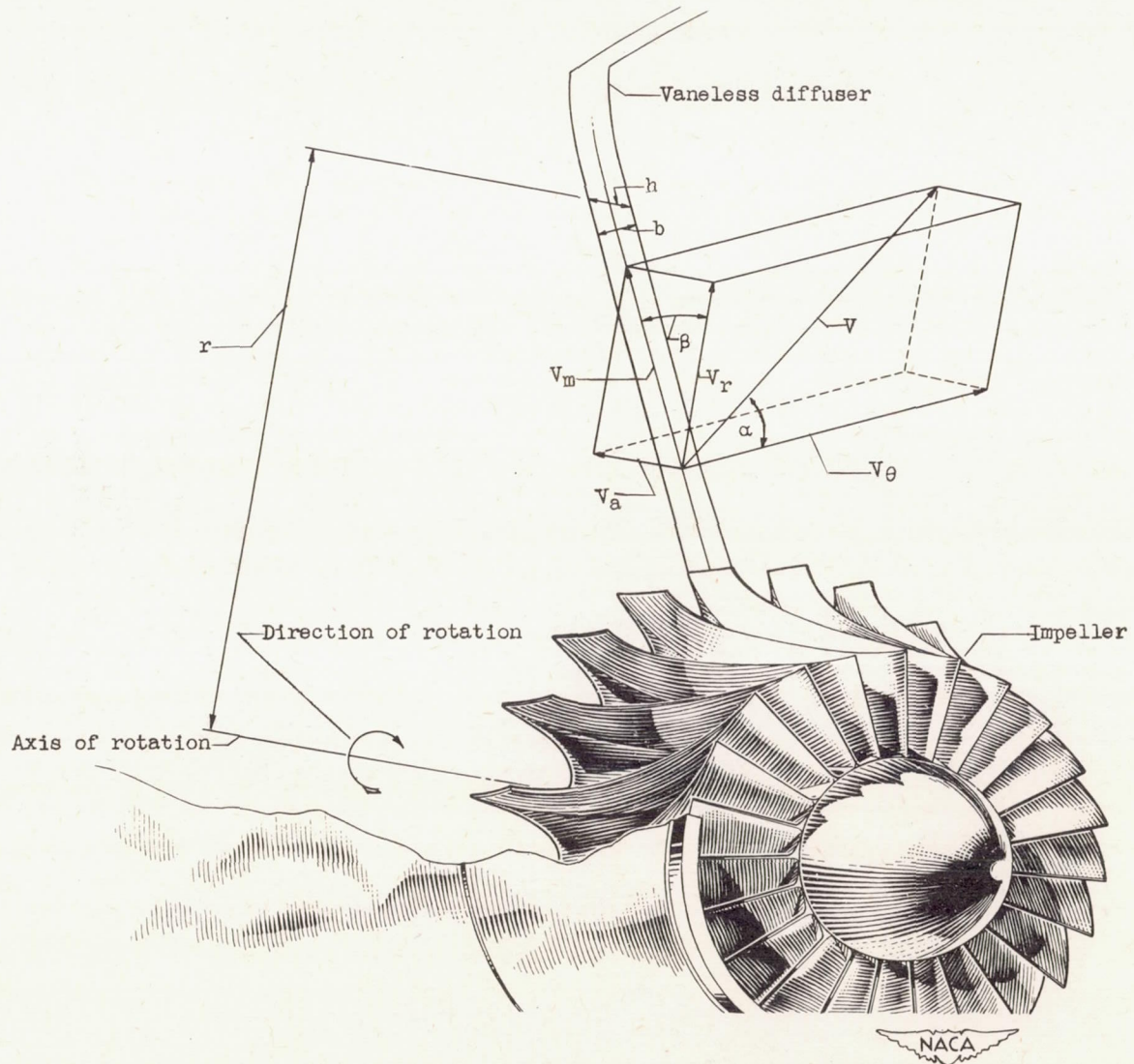


Figure 11. - Vector diagram of air flow through vaneless diffuser.